

PARALLEL COMPUTATION OF SMOKE MOVEMENT DURING A CAR PARK FIRE

Peter WEISENPACHER, Jan GLASA, Ladislav HALADA

Institute of Informatics

Slovak Academy of Sciences

Dúbravská cesta 9

845 07 Bratislava, Slovakia

e-mail: {upsyweis, glasa.ui, halada.ui}@savba.sk

Abstract. In this paper the use of Fire Dynamics Simulator (FDS) for parallel computer simulation of the smoke movement during a fire of two passenger cars in an underground car park is investigated. The simulations were executed on a high-performance computer cluster. A specific problem of FDS parallel computation using Message-Passing Interface (MPI) is a separate solution of governing equations on computational subdomains causing a loss of accuracy. Therefore, the impact of parallelisation on simulation accuracy in the case of using a greater number of computational cores of the computer cluster is studied with the aim to increase the computational performance and enable practical application of such simulations for fire safety measures. The geometrical model and material properties of the cars used in the simulation have been verified by a full-scale fire experiment in open air. We describe the results of a series of simulations of several fire scenarios with different numbers of parked cars and ventilation configurations and determine times and locations at which conditions in the car park become untenable for human life. The simulation indicates that proper ventilation prolongs tenable conditions by several minutes.

Keywords: Computer simulation, car park fire, FDS, parallelisation, high performance computing, cluster of computers

Mathematics Subject Classification 2010: 68U20, 65Y05

1 INTRODUCTION

The danger of car fire in transportation structures like tunnels and car parks, especially the fire smoke threat to human lives and health, requires a considerable effort to improve the design and functionality of ventilation systems. Because of a non-linear nature of fire, proper design of mechanical ventilation in car parks requires a careful evaluation of its possible harmful unintended effects. Although full-scale fire experiments are inevitable, their use is limited due to their high cost and insufficient flexibility. Recently, simulation systems based on Computational Fluid Dynamics (CFD) such as Fire Dynamics Simulator (FDS) have become an efficient tool for the design and evaluation of ventilation systems.

Several full-scale fire experiments examined the course of car fire under various conditions, measuring various physical quantities characterising the fire, such as the heat release rate, mass loss rate, heat flux and gas temperatures [7, 18, 20, 12, 11]. The fire of several cars and its impact on a car park structure was investigated in [26, 19]. In [2, 3] the temperature under ceiling, smoke back-layering and non-trivial flow patterns in the case of car park fire were studied by full-scale experiments and CFD simulations. In [5] the smoke movement in a car park with a jet fan ventilation under various conditions is investigated by general CFD software FLUENT.

One of the major problems of simulation of a car park fire is a realistic modelling of burning objects and their material properties, especially if the used computational mesh is too coarse to capture the objects properly. In [22] and [4] we have constructed an FDS model of fire of two passenger cars, whose reliability was confirmed by the results of a full-scale fire experiment conducted in 2009. This model enables to simulate the car park fire more realistically than by pool fire with prescribed HRR commonly used in the literature, especially if its mutual interaction with ventilation is crucial for the fire course. A similar approach was used in [13, 6] to model the influence of sprinklers on the fire. Realistic simulation often requires a significant computational performance; therefore the use of parallel simulation with a slightly lower accuracy is necessary in order to tackle the large compartment fire scenarios [23].

In this paper, we use our model of two passenger cars for the simulation of smoke propagation during a fire in an underground single-storey car park without and with ventilation. The focus is on the evaluation of tenability of conditions in the car park during the fire with respect to the temperature and soot visibility as well as on the description of growth of areas untenable for human life.

Large dimensions of the simulated structure require decomposing the computational domain into several computational meshes and realization of the computation in parallel. However, parallel computation influences the accuracy of obtained results. Therefore, the problem of simulation accuracy and performance must be dealt with the aim to achieve sufficient accuracy and to enhance the performance of parallel calculation on high-performance computer cluster. These issues are discussed here as well. Some preliminary results related to the research presented in this paper have been published in [25, 24].

The paper is structured as follows. In Section 2 the FDS simulation system is briefly characterised. Section 3 describes the full-scale fire experiment used for validation of the fire simulation of two passenger cars in open air and its computer simulation. In Section 4 parallel simulation of the fire of two cars from the previous section in a car park without ventilation is described. In Section 4.1 the influence of the number of cars parked in the car park on smoke propagation is investigated. The impact of parallelisation on the simulation results accuracy is discussed as well. Section 5 evaluates the performance of two ventilation systems during the two cars fire in the car park using high-performance simulations realised on computer cluster. The issues of parallel computation accuracy and applicability are discussed for the case in which a large number of computational meshes is used. Section 6 summarizes the main results of the paper.

2 FIRE DYNAMICS SIMULATOR

Fire Dynamics Simulator (FDS) is a CFD-based simulation system intended for modelling of fire-driven fluid flows developed by the National Institute of Standards and Technology (NIST), USA [8, 9]. FDS solves numerically a form of the Navier-Stokes equations appropriate for the low-speed, thermally-driven flow with an emphasis on the smoke and heat transport from fires. It also includes models of physical and chemical processes related to fire such as thermal radiation, pyrolysis, combustion of the pyrolysis products, conductive heat transfer and fire suppression by sprinklers.

The basic set of equations includes conservation equations for mass, species, momentum and energy [8]:

$$\frac{\partial \rho}{\partial t} + \nabla \cdot \rho \mathbf{u} = \dot{m}_b''' \quad (1)$$

$$\frac{\partial}{\partial t}(\rho Y_\alpha) + \nabla \cdot \rho Y_\alpha \mathbf{u} = \nabla \cdot \rho D_\alpha \nabla Y_\alpha + \dot{m}_\alpha''' + \dot{m}_{b,\alpha}''' \quad (2)$$

$$\frac{\partial}{\partial t}(\rho \mathbf{u}) + \nabla \cdot \rho \mathbf{u} \mathbf{u} + \nabla p = \rho \mathbf{f}_b + \nabla \cdot \boldsymbol{\tau}_{ij} \quad (3)$$

$$\frac{\partial}{\partial t}(\rho \mathbf{h}_s) + \nabla \cdot \rho \mathbf{h}_s \mathbf{u} = \frac{Dp}{Dt} + \dot{q}''' - \dot{q}_b''' - \nabla \cdot \dot{q}'' + \varepsilon \quad (4)$$

where $\dot{m}_b''' = \sum_\alpha \dot{m}_{b,\alpha}'''$ is the production rate of species by evaporating droplets or particles; ρ is the density; $\mathbf{u} = (u, v, w)$ is the velocity vector; Y_α , D_α , and $\dot{m}_{b,\alpha}'''$ are the mass fraction, diffusion coefficient, and the mass production rate of α^{th} species per unit volume, respectively; p is the pressure; \mathbf{f}_b is the external force vector; τ_{ij} is the viscous stress tensor; \mathbf{h}_s is the sensible enthalpy; and \mathbf{g} is the acceleration of gravity. The term \dot{q}''' is the heat release rate per unit volume from a chemical reaction and \dot{q}_b''' is the energy transferred to the evaporating droplets. The term \dot{q}'' represents the conductive and radiative heat fluxes. Note that $D()/Dt = \partial()/\partial t + \mathbf{u} \cdot \nabla()$. To these four equations, the equation of state for a perfect gas

$$p = \frac{\rho RT}{\bar{W}}, \quad (5)$$

in which R is the universal gas constant, T is the temperature and \bar{W} is the molecular weight of gas mixture, is added.

These equations must be simplified in order to filter out sound waves. The final numerical scheme is an explicit predictor-corrector finite difference scheme of the second order accuracy in space and time. The flow variables are updated in time using an explicit second-order Runge-Kutta scheme. The momentum equation is simplified and transformed into Poisson equation solved in every time step.

The input data for a simulation are given in a single text file of a prescribed format. It includes the description of the coordinate system, domain geometry, mesh resolution, obstacles, boundary conditions, material properties and other simulation parameters. The domain and all obstructions representing real objects (which can burn, heat up and conduct heat) should be rectangular and conformed to the underlying grid which represents an important limitation of the system. Boundary conditions are prescribed on walls and vents.

Source code of FDS 5.5.3 was compiled using the GNU 4.4.7 compiler (gfortran, gcc, OpenMP). There are three ways to execute FDS in parallel [23]: a parallel MPI (Message-Passing Interface) model designed for running on distributed memory systems, a multi-threading OpenMP model designed for running on shared memory systems and a hybrid MPI & OpenMP model designed for running on distributed shared memory systems. As demonstrated in [23], the parallel MPI model is the most efficient in FDS calculations; therefore we use it in this study (Open MPI version 1.6.3) [10]. The calculations were performed under Linux operating system on the SIVVP cluster at the Institute of Informatics, Slovak Academy of Sciences (Bratislava, Slovakia). It is an IBM dx360 M3 cluster with 54 computational nodes ($2 \times$ Intel E5645 @ 2.4 GHz CPU, 48 GB RAM) and 648 cores. All nodes are connected by the Infiniband interconnection network with the bandwidth of 40 Gbit/s per link and direction. Jobs were executed using the PBS (Portable Batch System) [14].

The strategy of parallel computation consists in decomposition of the computational domain into multiple computational meshes and computation of the flows in each mesh separately. Each computation is usually performed as an individual MPI process assigned to one CPU core. The values at mesh boundaries must be averaged in every time step in order to maintain the solution stability. Therefore, the way of the domain decomposition influences the accuracy of simulation results and must be examined carefully.

3 FULL-SCALE EXPERIMENT OF AUTOMOBILE INTERIOR FIRE AND ITS SIMULATION

In November 2009 we performed a full-scale experiment of a passenger car interior fire in open air and its spread onto another vehicle (see Figure 1). The experiment

was conducted in the testing facilities of the Secondary School of Fire Protection of the Ministry of Interior of the Slovak Republic in Povazsky Chlmec [15, 21, 4]. The fire was initiated in a new functional automobile Kia Cee'd. The right front and left rear side windows were broken in order to increase the oxygen supply. The second automobile was an older model of BMW, located lengthwise in the 50 cm distance. Gas temperatures inside and outside the cars were measured by thermocouples. The fire behaviour was observed and recorded by infra-red and digital cameras.



Figure 1. Full-scale fire experiment

The fire was ignited by burning of a small amount of gasoline (about 10 ml) placed onto the back seat behind the Kia driver's seat. The fire grew progressively and after 150 s the whole passenger compartment of Kia was burning. During the next minutes other windows were broken and the temperature inside the interior reached the value of 1 000 °C. After 7 minutes a rubber sealing of the nearest window of the BMW ignited. The fire was suppressed at the 12th minute of the experiment.

We used FDS for simulation of this fire scenario in order to validate the FDS representation of the cars and their material properties as well as the fire behaviour [22]. The 3 cm mesh resolution was used for the $576 \times 486 \times 240$ cm large computational domain. The total number of cells was 2 488 320. The cars were composed of metal sheets, rubber tyres and glass windows (see Figure 2). The second car included also a window rubber sealing at the place where the ignition of the BMW occurred during the experiment. Tabular values for properties of these materials were used. The model of cars also included the interior equipment such as seats, dashboard with a steering wheel and interior lining. We distinguished two interior materials namely 'UPHOLSTERY' for the seats and 'PLASTIC' for other equipment (see Figure 3 and Table 1) [22].

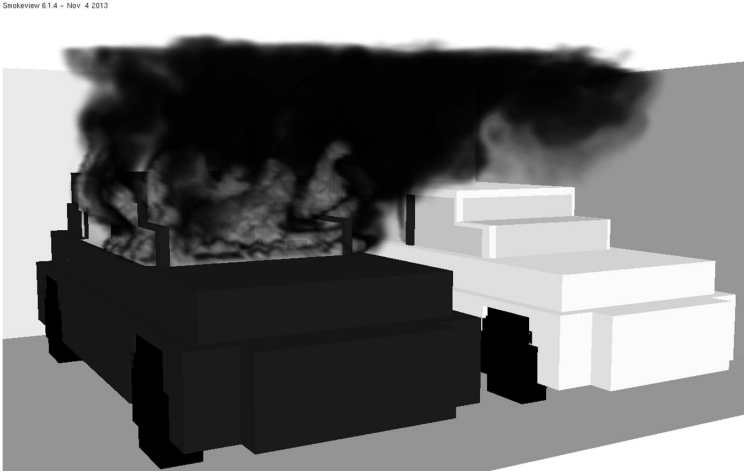


Figure 2. Fire simulation by FDS

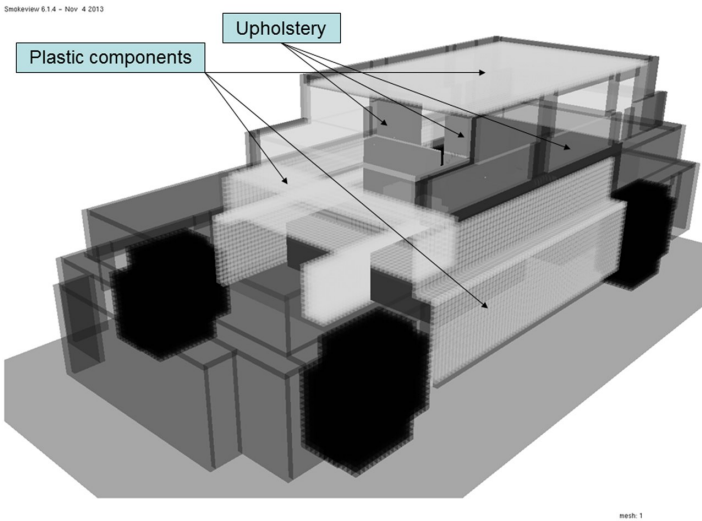


Figure 3. Passenger car interior materials

Type of Material	$T_{ign} [^{\circ}C]$	$H_v [kJ.kg^{-3}]$	$HRRPUA [kW.m^{-2}]$	$\rho [kg.m^{-3}]$
'UPHOLSTERY'	370	4000	200	80
'PLASTIC'	440	4000	250	930

Table 1. Material properties of dominant materials of the interior

The fire behaviour in the simulation was qualitatively very similar to the experiment and the simulated temperatures were in good correspondence with experimental measurements. The 3 MW HRR peak as well as the influence of the windows breakage succession on the fire course are consistent with [12] as well.

4 SIMULATION OF CAR PARK FIRE

We constructed an FDS model of an underground car park with the dimensions $23.04 \times 38.88 \times 3.0$ m (the total area of 895.8 m^2) with parking places for 24 cars (see Figure 4).

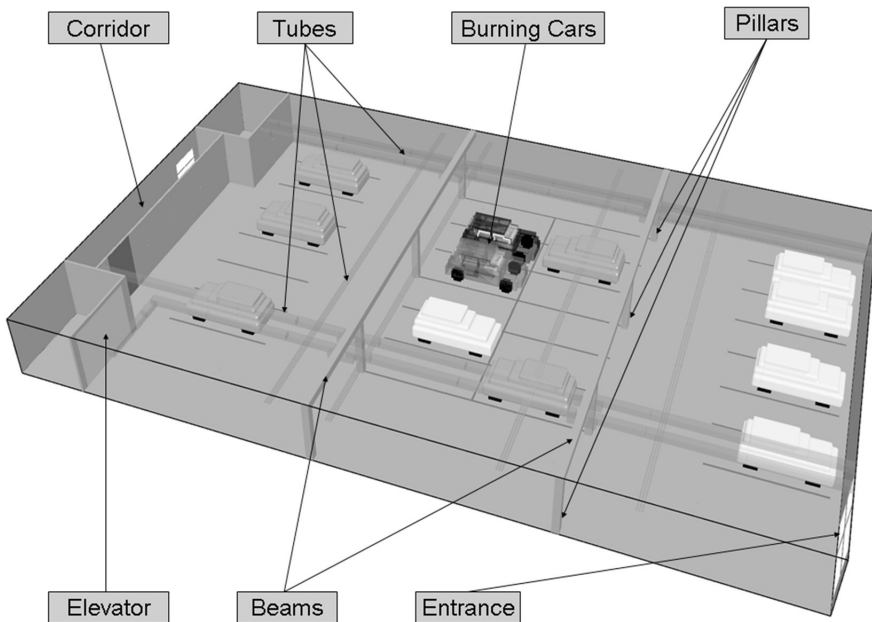


Figure 4. Car park scheme

The car park includes two concrete beams under the ceiling and 8 columns of 36 cm thickness. The 3.96 m wide entrance to the car park located in its right part is connected with particular parking places by an access road. The car park includes two burning cars in its middle part and 10 non-flammable randomly parked cars. The left part of the car park includes the elevator door and the corridor leading inside the building. The tube system located under the ceiling consists of tubes of 6 cm and 36 cm thickness. We consider a fire source of 72.9 kW HRR located on the driver's seat of the right car under its broken left window [25, 24].

As the 3 cm computational mesh resolution is too fine for the simulation of fire in such large compartment, the influence of coarser grid on the simulation accuracy

was tested in [25]. The simulation with the 6 cm mesh resolution gives reasonable accuracy if no mesh boundary lies between the burning cars. Therefore, the domain is decomposed in accordance with these observations. The numbers of used meshes is 144 (see Figure 5). The simulation includes $384 \times 648 \times 50$ cells (the total cell number is 12 441 600). The default FDS radiation model and Large Eddy Simulation [9] are used in the simulation. The ambient temperature of 20°C is set. Boundary conditions are modelled by 10 cm thick concrete layer; the entrance is modelled by the ‘OPEN’ boundary condition. The soot yield of 0.1 of the dominant chemical reaction is set in the simulation. The calculations of 600 s of fire were performed. The total computational time is about 1 day.

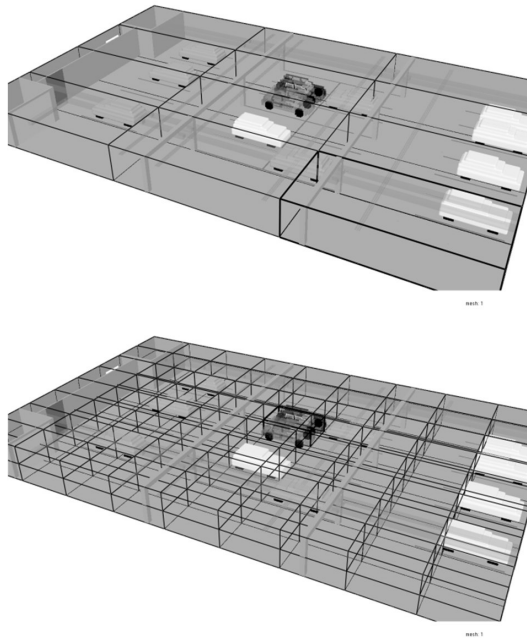


Figure 5. 12M and 144M computational domain decompositions

The simulation aims to determine the time when conditions in particular locations of the car park become untenable for human life. The International Fire Engineering Guidelines [1] defines untenable conditions as “environmental conditions associated with a fire in which human life is not sustainable” – in other words, conditions that cause death. A comprehensive review of exposure thresholds that cause incapacitation and death can be found in [17]. A brief description can be found in [16]. In our study the untenable conditions are assessed with respect to the temperature (the temperature greater than 70°C is considered untenable) and soot visibility (visibility less than 10 m is considered untenable). The untenable conditions are measured at human head level (1.62 m height). The temperature threshold

corresponds to humid air conditions and long exposure duration. The visibility threshold corresponds to large compartments. Fulfilment of such criteria enables safe evacuation of people from the car park. Other tenability criteria (fractional effective dose, radiant heat) are not evaluated.

The simulated fire behaviour is qualitatively similar to the car fire simulation in open air described in [23], although its course is accelerated because of the more intensive fire source. In addition, some new phenomena appear due to specific geometry of the car park. The air flow leading from the elevator door to the fire is formed, accelerating burning of the second car. In order to evaluate this phenomenon we performed an additional simulation in which the computational domain does not include walls. The domain dimensions are $8.64 \times 8.64 \times 3.0$ m. It includes concrete floor and ceiling, while other domain boundaries are represented by the ‘OPEN’ boundary conditions. The HRR value of 5 MW corresponding to a fully developed fire of both cars interiors is achieved at the 419th s in the car park fire simulation. In the simulation not including walls it is achieved at the 527th s, as any similar horizontal air flows cannot be formed, see Figure 6.

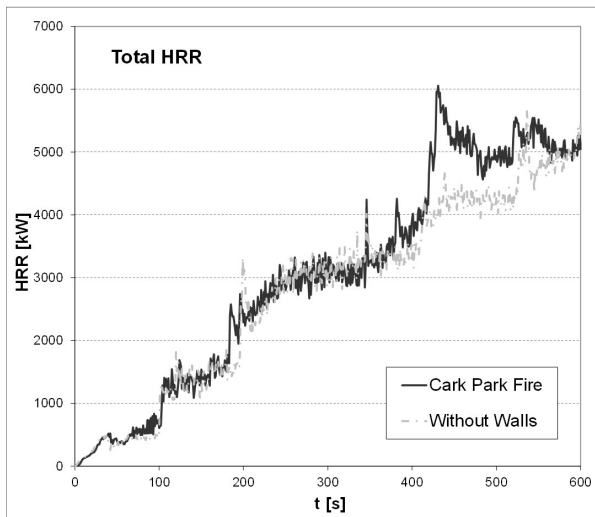


Figure 6. HRR of the car park fire

The smoke movement is illustrated in Figure 7. Figure 8 shows a gas velocity slice at head level. In Figures 9 and 10 the visibility and temperature slices crucial for determination of the time when untenable conditions occur are shown.

At first smoke spreads under the ceiling in all directions and is temporarily contained in the middle part of the car park by both beams. After reaching the walls it starts to descend and then spreads in opposite directions. The first significant drop of visibility occurs near the entrance and near the elevator (see Figure 9). In these locations conditions become untenable between the 100th and 130th s. During

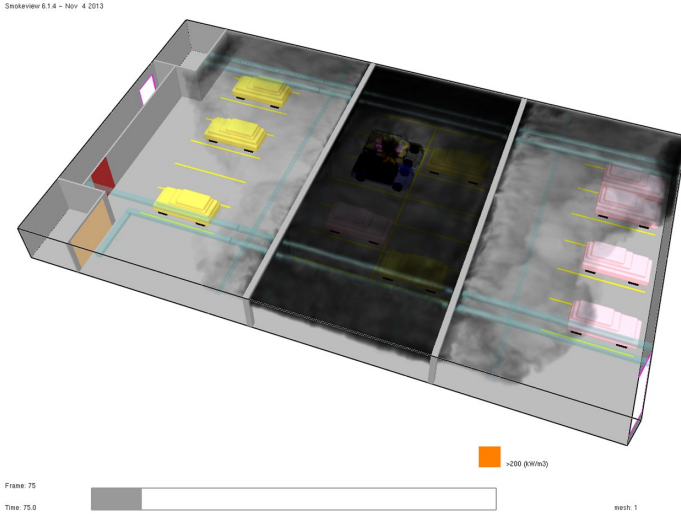


Figure 7. Smoke movement at the 75th s

the next minute the areas of untenability grow and afflict about one half of the compartment. After another half minute, visibility conditions become untenable in the whole car park. The untenability caused by the temperature increase is delayed significantly (see Figure 10). Between the 6th and 7th minute, conditions are untenable near the entrance and the elevator. After the next minute they are

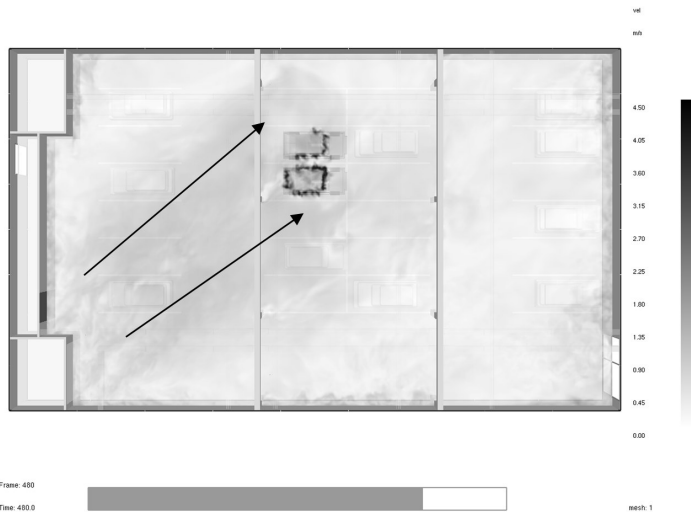


Figure 8. Air velocity slice at head level at the 480th s (the values vary from 0 to 4.5 m.s⁻¹)

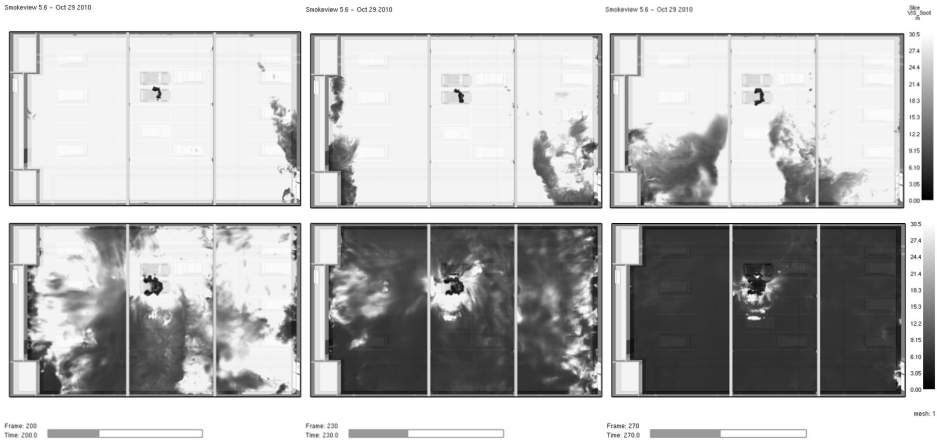


Figure 9. Visibility slices at head level at the 100th s, 130th s, 160th s, 200th s, 230th s and 270th s (the values vary from 0 to 30 m)

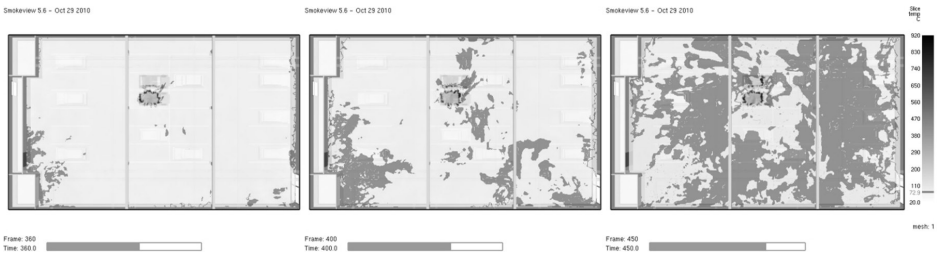


Figure 10. Temperature slices at head level at the 360th s, 400th s and 450th s (the threshold value is 72.9 °C)

untenable in the whole compartment. Note that the temperature tenability limit of 120 °C for firefighting operations (up to 10 minute duration) was not achieved in the car park during the whole period of simulation.

4.1 Fire Simulation in Full and Empty Car Park

As parked cars influence the air flows, it is useful to quantify the impact on the smoke movement. The averaged visibility S_{avg} at head level is used as a measure of this phenomenon, although it does not reflect the local character of untenability conditions. Taking into account a simple shape of the curve of this quantity, the time average of this quantity over 600s of simulation S_t is an even more simplified aggregate value characterising the smoke propagation. We compared the results of the simulation (12 cars) described in the previous section with the simulations in the full (24 cars) and empty (2 cars) car park.

There is a specific source of errors caused by parallelisation in simulations. The sequential calculation is the most accurate and the accuracy of parallel calculations has a tendency to decrease with increasing number of computational meshes. However, the sequential calculation cannot be performed due to extremely long CPU time. In order to evaluate the 144 M simulations accuracy, we performed 12 M simulations in which the computational domain was decomposed into 12 meshes (see Figure 5). Smaller accumulation of errors on mesh boundaries makes the 12 M simulations more accurate requiring a realistic CPU times. Therefore, in those cases where the 144 M simulations accuracy must be tested, the 12 M simulations are used as the most suitable basis for the comparison. The total computational time is about 1 to 1.5 day for 144 M simulations and 9 to 11 days for 12 M simulations.

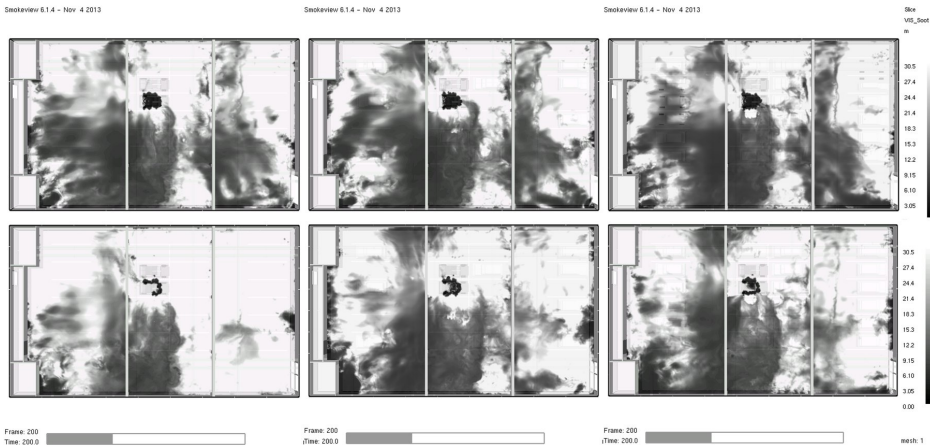


Figure 11. Visibility slices at head level after 200s for the fire scenarios with empty, half-full and full car park (left to right) for the 12 M (the first row) and 144 M (the second row) simulations

Our previous results [25] using 144 M simulations indicated that the presence of cars accelerates the rise of untenability. The drop of tenability occurred sooner in the full car park ($S_t = 10.77$ m) than in the empty car park scenario ($S_t = 11.34$ m) with the time difference of about dozens of seconds. However, more precise 12 M simulations do not confirm this effect. The comparison of 12 M and 144 M simulations for the empty and full car parks (Figures 11 and 12) indicates that the difference between the simulations is caused by a lesser accuracy of 144 M simulations rather than by the number of parked cars. The difference between the empty ($S_t = 10.76$ m) and full ($S_t = 10.66$ m) car park scenario is small for the 12 M simulations. In spite of this, small local differences of smoke patterns caused by the presence of cars can be observed as well (Figure 11).

The visibility slices in Figure 11 are very similar except the one related to the 144 M simulation for empty car park. To interpret the difference of the 4th picture

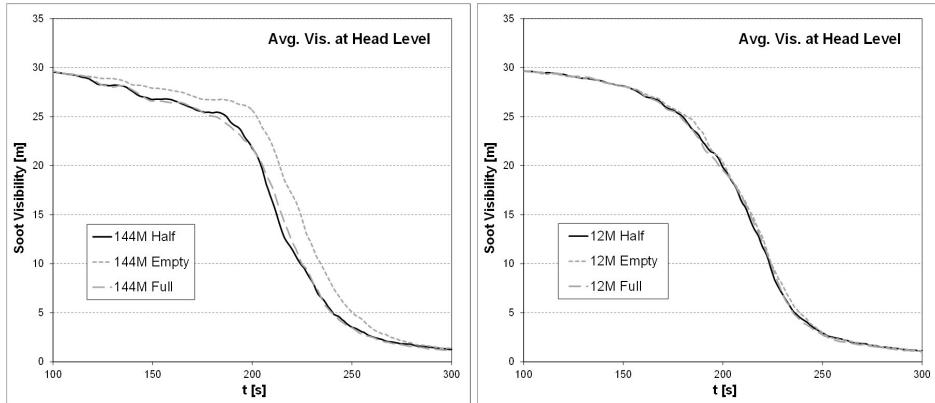


Figure 12. Averaged visibility at head level for the fire scenario with the half-full, full and empty car park, according to the 144 M and 12 M simulations

in Figure 11, one must consider the overall forming of smoke layer at the given time. The similar descending smoke layer is formed in all six studied scenarios, however, in the 144 M empty scenario the smoke layer descent is slightly delayed. At the 200ths some parts of the layer are located slightly over the head level, which leads to different pattern in the 4th picture of Figure 11 than in other scenarios, in which the layer has already reached the head level. In order to evaluate the difference between the simulations, we focus on delays of smoke layer movement in given scenarios. The 144 M empty scenario delay is about 12 s (see Figure 12). Such delay seems to be tolerable, taking into account the significant performance increase of the 144 M simulation in comparison with the 12 M simulation. Although the 144 M simulations tend to slightly overestimate differences between scenarios with different number of cars, the simulation accuracy is sufficient for practical purposes.

5 SIMULATION OF CAR PARK FIRE WITH VENTILATION

The impact of ventilation on the smoke movement is simulated using two metal ductwork systems for mechanical smoke extraction (see Figure 13). The first simulation scenario (D1) uses 9 inlet fans located in proximity of the elevator and the corridor entrance, and 9 outlet fans almost regularly distributed within the ductwork system. Both the inlet and outlet fans are represented by 96×48 cm surfaces with prescribed normal air velocity. The second scenario (D2) uses 9 inlet fans (three of them have a different position than in D1) and 12 outlet fans. The D2 configuration is chosen with the aim to direct the air flow below the ceiling through the entrance by the specific location of outlet fans and to use the car park entrance as an extract or supply opening. Several values of the inlet and outlet velocity are tested, including the values below 2 m.s^{-1} which do not disrupt the hot layer. The averaged visibility, the time averaged visibility and the visibility near the corridor door are

used to evaluate the efficiency of both ventilation systems. The results of the 144 M simulation of D1 and D2 are presented in Tables 2 and 3.

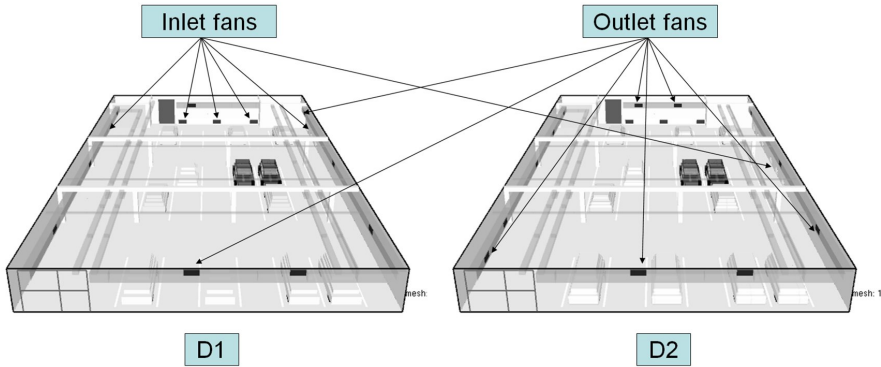


Figure 13. Two configurations of ductwork ventilation system

From the point of view of the time averaged visibility, the D1 configuration is the most efficient if the $(1.5 \text{ m.s}^{-1}, 3 \text{ m.s}^{-1})$ combination of fan velocities is used, while the $(2 \text{ m.s}^{-1}, 4 \text{ m.s}^{-1})$ combination is slightly less efficient. However, the latter one provides slightly better visibility results for the final fire phase when the HRR value increases. The combinations with higher outlet velocities disrupt the hot layer and their results are worse, although they produce the best visibility results at the 600th s of the fire, i.e. in that phase of the fire when the hot layer is below the head level anyway. Another advantage of these combinations is a better visibility near the entrance in the latter phase of the fire, which enables a better access of fire fighters to the fire source. The combinations with low velocities leave the hot layer intact which leads to better visibilities in an early phase of the fire, while in later phases the rate of the smoke removal is not sufficient. The combinations with the 9 m.s^{-1} outlet velocity and to a lesser extent also the $(2 \text{ m.s}^{-1}, 4 \text{ m.s}^{-1})$ and $(1.5 \text{ m.s}^{-1}, 3 \text{ m.s}^{-1})$ combinations give good results of visibility near the corridor door which makes evacuation easier.

The best results are obtained for those combinations, in which the outlet velocity is slightly higher than the inlet velocity. A similar behaviour can be observed for the D2 configuration, where the $(1.5 \text{ m.s}^{-1}, 2 \text{ m.s}^{-1})$ and $(2 \text{ m.s}^{-1}, 3 \text{ m.s}^{-1})$ combinations lead to the best time averaged visibility. The highest visibility in the tested D2 configurations is higher than in the D1 configurations (20.6 m vs. 18.9 m).

Based on the results listed in Tables 2 and 3, the values of the time dependent inlet and outlet velocities can be proposed with the aim to optimize the smoke extraction during the fire. The velocity values at the 180th, 360th and 600th s are shown in Table 4 while other values are linearly interpolated. For 144M simulation, the values 19.5 m and 21.1 m of the time averaged visibility for the D1 and D2 configuration are achieved, respectively. Time behaviour of the visibility of the

SC	v_{in} [m.s ⁻¹]	v_{out} [m.s ⁻¹]	Q_{out} [m ³ h ⁻¹]	S_{180s} [m]	S_{360s} [m]	S_{600s} [m]	S_t [m]	S_{door} [m]
D0	–	–	–	25.4	0.7	0.3	10.8	8.9
D1	0.0	1.5	22 395	26.6	3.2	0.5	13.2	12.5
D1	1.5	1.5	22 395	27.7	7.6	1.2	15.0	11.5
D1	1.5	2.0	29 860	28.5	12.9	2.4	17.3	12.7
D1	1.5	3.0	44 790	27.9	15.2	5.0	18.9	15.6
D1	1.5	4.0	59 720	27.3	9.2	4.3	16.4	14.4
D1	1.5	6.0	89 580	26.7	9.5	2.9	16.0	13.5
D1	1.5	9.0	134 369	23.5	10.2	5.9	16.1	15.5
D1	2.0	2.0	29 860	27.0	7.5	1.8	15.0	11.8
D1	2.0	3.0	44 790	27.9	13.2	4.9	18.0	12.2
D1	2.0	4.0	59 720	27.4	13.7	6.2	18.4	15.4
D1	2.0	6.0	89 580	26.8	9.6	3.4	16.4	13.6
D1	2.0	9.0	134 369	24.2	10.9	6.1	16.4	16.1
D1	2.5	4.0	59 720	27.1	12.9	6.0	17.8	12.4
D1	3.0	4.0	59 720	24.8	9.2	3.9	15.4	11.2
D1	3.0	6.0	89 580	26.4	9.0	6.1	16.3	13.7
D1	3.0	9.0	134 369	25.0	11.6	5.7	17.1	15.9

Table 2. Simulation configurations (SC) and the related values of the inlet velocity v_{in} , the outlet velocity v_{out} , the extract volume flux Q_{out} ; the average visibility S_{180s} , S_{360s} and S_{600s} after the 180th s, 360th s and 600th s, respectively; the time averaged visibility S_t and the time averaged visibility near the door S_{door} (the best values are highlighted by bold). D0 denotes the simulation without ventilation.

optimal simulations and the D1 (3 m.s⁻¹, 9 m.s⁻¹) simulation are shown in Figure 14. Visibility slices at selected times are illustrated in Figure 15.

The D1 configuration prolongs averaged tenability conditions by 4 to 5 minutes while the D2 configuration maintains tenability conditions for the whole 10-minute period of the fire (Figure 14). D2 also preserves a better visibility near the corridor door (see Figure 15).

Flow patterns at head level of the selected simulations are different (Figure 16). In D1-optimal the inlet fans produce two air flows directed away from the left corners of the car park, merging and creating a horizontal air flow in the car park slice, which is then slightly diverted upwards due to its interaction with fire. It creates a counter-clockwise swirl in the left part of the car park persisting up to approximately the 300th s of the fire. In the later phase of the fire the flow is diverted and leads to the upper right area in the slice.

In D2-optimal a large counter-clockwise swirl is created inside the car park. The swirl afflicts the major part of the compartment and persists until the end of the simulation. It removes smoke through the entrance and delivers it to the extract fans ensuring very efficient smoke extraction and creating a large smoke-free zone in the central part of the car park. In general, the time and spatial pattern of D1

SC	v_{in} [m.s ⁻¹]	v_{out} [m.s ⁻¹]	Q_{out} [m ³ h ⁻¹]	S_{180s} [m]	S_{360s} [m]	S_{600s} [m]	S_t [m]	S_{door} [m]
D2	1.5	1.5	29 860	28.5	13.8	6.7	19.0	13.7
D2	1.5	2.0	39 813	28.3	17.8	7.6	20.6	21.1
D2	1.5	3.0	59 720	28.1	11.2	6.0	17.8	16.1
D2	1.5	4.0	79 626	26.9	11.3	4.1	17.0	13.9
D2	1.5	6.0	119 439	24.4	11.0	5.5	16.7	14.5
D2	1.5	9.0	179 159	19.4	8.9	5.6	14.6	13.9
D2	2.0	2.0	39 813	27.9	12.5	8.3	18.8	13.8
D2	2.0	3.0	59 720	26.9	14.4	9.7	19.5	16.6
D2	2.0	4.0	79 626	26.8	10.3	4.6	16.8	14.8
D2	2.0	6.0	119 439	25.4	11.6	5.8	17.4	14.7
D2	2.0	9.0	179 159	21.2	10.4	6.7	15.3	14.6
D2	2.5	3.0	59 720	25.6	12.4	9.0	18.1	13.3
D2	2.5	4.0	79 626	26.0	10.1	7.4	16.7	13.2
D2	2.5	6.0	119 439	25.5	12.1	6.2	17.6	15.7
D2	2.5	9.0	179 159	21.1	10.7	7.0	15.7	14.4
D2	3.0	3.0	59 720	24.8	9.6	6.5	16.2	12.4
D2	3.0	4.0	79 626	23.6	10.5	8.1	16.4	12.3
D2	3.0	6.0	119 439	25.2	11.1	6.4	17.1	16.8
D2	3.0	9.0	179 159	21.3	10.4	6.9	16.1	14.7

Table 3. Simulation configurations (SC) and the related values of the inlet velocity v_{in} , the outlet velocity v_{out} , the extract volume flux Q_{out} ; the average visibility S_{180s} , S_{360s} and S_{600s} after the 180th s, 360th s and 600th s, respectively; the time averaged visibility S_t and the time averaged visibility near the door S_{door} (the best values are highlighted by bold).

Conf	S_t [m] 12 M/144 M	$v_{180s,in}$ [m.s ⁻¹]	$v_{180s,out}$ [m.s ⁻¹]	$v_{360s,in}$ [m.s ⁻¹]	$v_{360s,out}$ [m.s ⁻¹]	$v_{600s,in}$ [m.s ⁻¹]	$v_{600s,out}$ [m.s ⁻¹]
D1-optimal	18.4/19.5	1.5	2.0	1.5	3.0	2.0	4.0
D2-optimal	20.8/21.1	1.5	2.0	1.5	2.0	2.5	3.0

Table 4. Values of optimized time dependent inlet and outlet velocities

is more variable and complicated. Note that a better visibility in the D2 scenario is achieved because of the specific configuration of burning cars. Air flows created by D2 avert the flames of the first car fire from the second car. The ignition of the second car occurs later and the smoke production is less intensive. In general, D2 is not more efficient than D1.

In D1 (3 m.s⁻¹, 9 m.s⁻¹) the higher extraction velocities create a strong clockwise flow leading from the entrance in the proximity of the car park walls.

The 144 M simulations increase the computational performance significantly, about 10 times. They provide reasonable accuracy of description of the main features of the tested fire scenarios. In Figure 14 it can be seen that the differences between

the simulations 12M and 144M increase with increasing fan velocity. It indicates that faster flows result in worse simulation accuracy if a higher number of meshes is used.

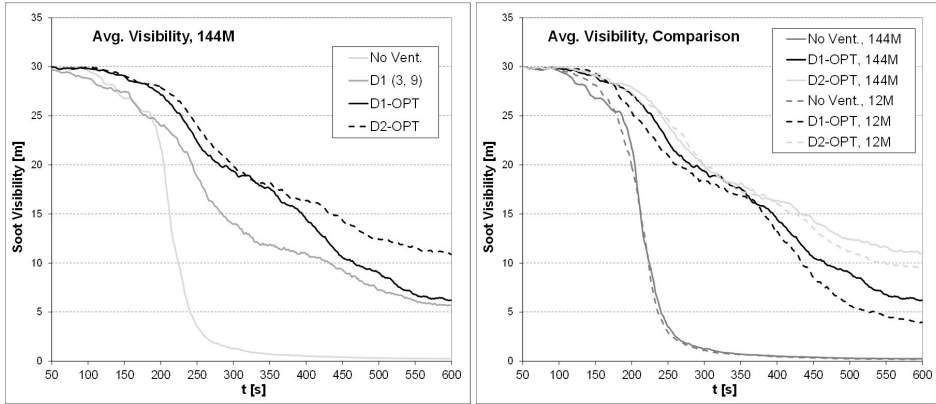


Figure 14. Averaged visibility at head level for several fire scenarios with ventilation for the 12M and 144M simulations

Analysis of the smoke layer behaviour simulated by the 12M and 144M simulations shows that both are qualitatively very similar (see Figure 15, rows 1, 2). From the point of view of the time shift between the simulations, one can see that the simulations without ventilation give almost the same behaviour. The faster air flows in optimal ventilation scenarios increase errors of the 144M simulations, however, the time shift is usually below 20s and the relative difference (in comparison with 12M) is less than 10% for the most part of fire duration. The relative differences increase after 450s with increasing flow velocity, however, at that time untenable visibility values have been already reached in the D1-optimal scenario. In the D2-optimal scenario the differences are relatively small, although very small decrease of the 144M average visibility curve leads to the overestimation of the time at which untenable conditions occur.

For these reasons the 144M simulations seem to provide reasonable accuracy of prediction of main features of the smoke behaviour for practical purposes (especially in the early phase of fire) as well as the time at which untenable conditions can be expected. Note that errors arise at boundaries of all 144 meshes and they cumulate, therefore, some differences in the simulation results are natural. Based on our experience, these errors increase relatively randomly with increasing mesh number and there is no clear pattern to describe them.

6 CONCLUSION

In this paper, the FDS model of a fire of two passenger cars is used to simulate the movement of smoke in an underground car park with the aim to determine the

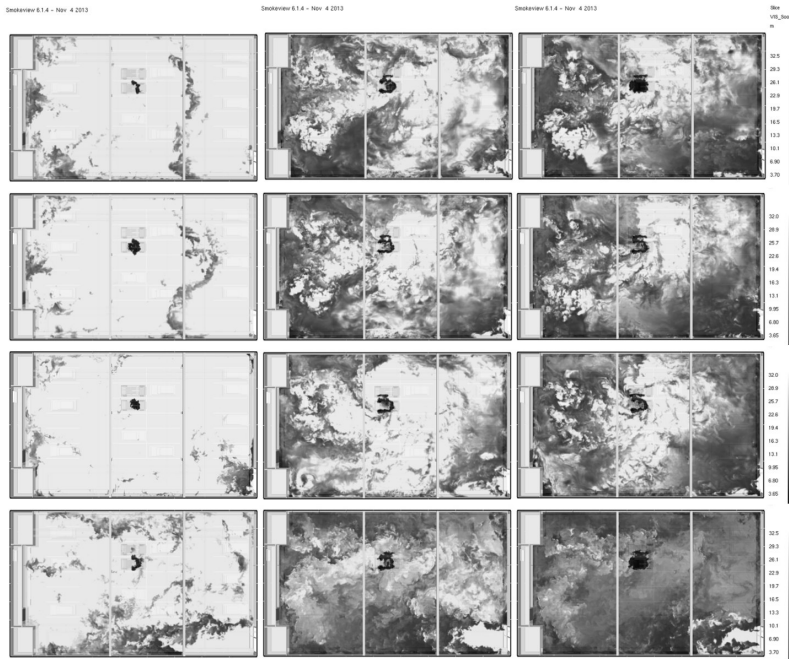


Figure 15. Visibility slices at head level after the 160th s, 270th s and 360th s for the fire scenarios with the D1-optimal (144 M), D1-optimal (12 M), D2-optimal (12 M) and D1 (3 m.s^{-1} , 9 m.s^{-1}) (144 M) ductwork ventilation

time at which conditions untenable for human life arise. In the most endangered locations they occur between the 100th and 130th s of fire. After another 100 s the conditions become untenable in the whole car park. The untenability caused by the temperature occurs after 400 s of fire. The effect of cars parked in the car park without ventilation on the smoke movement is evaluated and small differences of the averaged visibility are ascertained. Simulations using a higher number of computational meshes tend to overestimate differences between the empty and full car park scenario.

Several ductwork ventilation configurations with different inlet and outlet fan velocities are studied. Their impact on the air flow and the soot visibility decrease is examined determining the optimal fan velocities. The optimized scenarios show the averaged prolongation of tenability conditions by 4 to 6 minutes and the prolongation by about 2 to 6 minutes in the areas important for safe evacuation of people (areas in the proximity of the corridor door).

The impact of domain decomposition into 12 and 144 computational meshes used in the simulation parallelisation is evaluated. The calculations with 144 meshes increase computational performance significantly, about 10 times. Faster air flows in the car park result in a worse simulation accuracy if a higher number of meshes

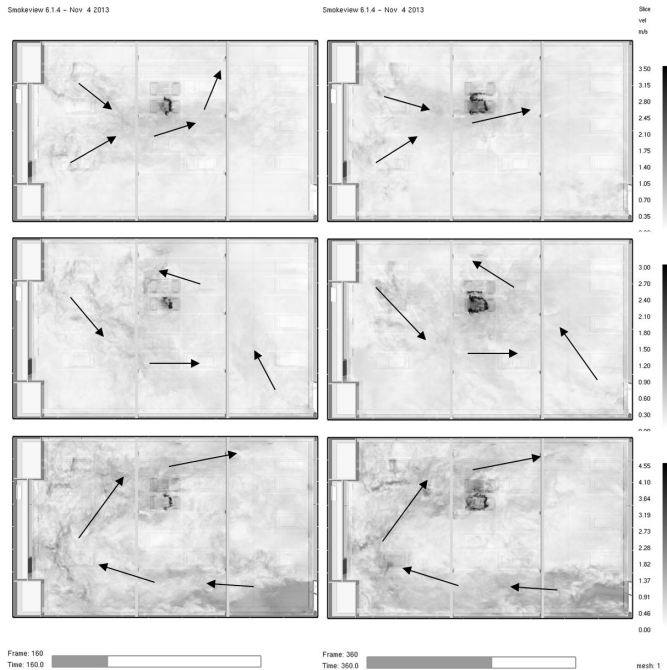


Figure 16. Velocity slices at head level at the 160ths and the 360ths for fire scenarios with the D1-optimal (12 M), D2-optimal (12 M) and D1 (3 m.s^{-1} , 9 m.s^{-1}) (144 M) ductwork ventilation

is used. Although the 144 M simulations are less accurate than the simulations with 12 meshes, they provide reasonable description of the smoke movement for practical purposes of fire safety.

The results of this study demonstrate the usefulness and applicability of the two passenger car model for testing the fire safety issues in car parks for fire scenarios where mutual interaction between air flow and fire must be taken into account. They allow proposing and testing measures for improvement of fire safety in car parks. A further research of the impact of various placements of burning cars and their numbers on smoke movement would be very useful.

Acknowledgement

The authors would like to thank P. Polednak, J. Svetlik, M. Simonova and J. Flachbart for organizing the fire experiments and M. Dobrucky, J. Astalos, P. Slizik and V. Sipkova for technical support for SIVVP cluster computing. This paper was partially supported by the Slovak Science Foundation VEGA (project No. 2/0184/14) and the Slovak Research and Development Agency APVV (project No. APVV-15-0340).

REFERENCES

- [1] ABCB, International Fire Engineering Guidelines, Australian Building Codes Board, Canberra, Australia, 2005.
- [2] DECKERS, X.—HAGA, S.—SETTE, B.—MERCİ, B.: Smoke Control in Case of Fire in a Large Car Park: Full-Scale Experiments. *Fire Safety Journal*, Vol. 57, 2013, pp. 11–21.
- [3] DECKERS, X.—HAGA, S.—TILLEY, N.—MERCİ, B.: Smoke Control in Case of Fire in a Large Car Park: CFD Simulations of Full-Scale Configurations. *Fire Safety Journal*, Vol. 57, 2013, pp. 22–34.
- [4] HALADA, L.—WEISENPACHER, P.—GLASA, J.: Computer Modelling of Automobile Fires. Chapter 9. In: Liu, C. (Ed.): *Advances in Modeling of Fluid Dynamics*. InTech Publisher, Rijeka, 2012, pp. 203–228.
- [5] HEGEMAN, S. T. G. D.: Smoke Movement in Fire Situations. CFD-Utilization in Car Park Fleerde. Technical University of Eindhoven, 2008.
- [6] HEINISUO, M.—PARTANEN, M.: Modeling of Car Fires with Sprinklers. Research report No. 161. Tampere University of Technology, Department of Civil Engineering, 2013, pp. 70.
- [7] MANGS, J.—KESKI-RAHKONEN, O.: Characterization of the Fire Behaviour of a Burning Passenger Car. Part I: Car Fire Experiments. *Fire Safety Journal*, Vol. 23, 1994, No. 1, pp. 17–35.
- [8] MCGRATTAN, K.—HOSTIKKA, S.—FLOYD, J.—BAUM, H.—REHM, R.—MELL, W.—MCDERMOTT, R.: Fire Dynamics Simulator (Version 5). Technical Reference Guide. Vol. 1, Mathematical Model, NIST Special Publication 1018-5, NIST, Gaithersburg, MD, USA, 2009.
- [9] MCGRATTAN, K.—KLEIN, B.—HOSTIKKA, S.—FLOYD, J.: Fire Dynamics Simulator (Version 5): User's Guide. NIST Special Publication 1019-5, NIST, Gaithersburg, MD, USA, 2009.
- [10] Open MPI – A High Performance Message Passing Library. Available on: <http://www.open-mpi.org/>.
- [11] OKAMOTO, K.—OTAKE, T.—MIYAMOTO, H.—HONMA, M.—WATANABE, N.: Burning Behaviour of Minivan Passenger Cars. *Fire Safety Journal*, Vol. 62, 2013, pp. 272–280.
- [12] OKAMOTO, K.—WATANABE, N.—HAGIMOTO, Y.—CHIGIRA, T.—MASANO, R.—MIURA, H.—OCHIAI, S.—SATO, H.—TAMURA, Y.—HAYANO, K.—MAEDA, Y.—SUZUKI, J.: Burning Behaviour of Sedan Passenger Cars. *Fire Safety Journal*, Vol. 44, 2009, pp. 301–310.
- [13] PARTANEN, M.—HEINISUO, M.: Car Fires with Sprinklers: A Study on the Eurocode for Sprinklers. Proceedings of International Conference Applications of Structural Fire Engineering, Prague, Czech Republic, 2013, pp. 23–28.
- [14] PBS – Portable Batch System. Available on: <http://www.mcs.anl.gov/research/projects/openpbs/>.

- [15] POLEDNAK, P.: Experimental Verification of Automobile Fires. Proceedings of the 4th International Conference on Fire Safety and Rescue Services, Zilina, Slovakia, 2010, pp. 248–255 (in Slovak).
- [16] Practice Note for Tenability Criteria in Building Fires. Society of Fire Safety, Engineers Australia, April 2014.
- [17] PURSER, D. A.: Assessment of Hazards to Occupants from Smoke, Toxic Gases and Heat. In: DiNenno, P. J. (Ed.): *The SFPE Handbook of Fire Protection Engineering*. 4th Edition, National Fire Protection Association, Quincy, MA 02269, 2009, pp. 2/96–2/193.
- [18] SHIPP, M.—SPEARPOINT, M.: Measurements of the Severity of Fires Involving Private Motor Vehicles. *Fire and Materials*, Vol. 19, 1995, No. 3, pp. 143–151.
- [19] SCHLEICH, L. B.—CAJOT, L. G.—PIERRE, M.—BRASSAUER, M.—FRANSSSEN, J. M.—KRUPPA, J.—JOYEUX, J.—TWILT, L.—VAN OERLE, J.—AURTENETXE, G.: Development of Design Rules for Steel Structures Subjected to Natural Fires in Closed Car Parks. Luxembourg, European Commission, 1999.
- [20] STEINERT, C.: Experimentelle Untersuchungen zum Abbrand- und Feuerübersprungs-Verhalten von Personenkraftwagen. *Vfbd-Zeitschrift*, Vol. 49, 2000, No. 4, pp. 163–172 (in German).
- [21] SVETLIK, J.—FLACHBART, J.: Skip Fire from Vehicle to Vehicle – Experiment. In: *Book of Proceedings of the 3rd International Scientific Conference on Safety Engineering and the 13th International Scientific Conference Fire and Explosion Safety*, The Higher Education Technical School of Professional Studies, Novi Sad, October 18–19, 2012, pp. 113–118.
- [22] WEISENPACHER, P.—GLASA, J.—HALADA, L.: Automobile Interior Fire and Its Spread to an Adjacent Vehicle: Parallel Simulation. *Journal of Fire Sciences*, Vol. 34, 2016, No. 4, pp. 305–322, DOI: 10.1177/0734904116647972.
- [23] WEISENPACHER, P.—GLASA, J.—HALADA, L.—VALASEK, L.—SIPKOVA, V.: Parallel Computer Simulation of Fire in Road Tunnel and People Evacuation. *Computing and Informatics*, Vol. 33, 2014, No. 6, pp. 1237–1268.
- [24] WEISENPACHER, P.—HALADA, L.—GLASA, J.—ASTALOS, J.: Influence of Parked Cars on Smoke Propagation During Car Park Fire. Proceedings of the 26th European Modeling and Simulation Symposium, Bordeaux, France, 2014, pp. 384–391.
- [25] WEISENPACHER, P.—HALADA, L.—GLASA, J.—SLIZIK, P.: Smoke Propagation in Car Park Fire: A Parallel Study. Proceedings of Eight Mediterranean Combustion Symposium, Cesme, Izmir, Turkey, September 8–13, 2013.
- [26] ZHAO, B.—KRUPPA, J.: Structural Behaviour of an Open Car Park under Real Fire Scenarios. *Fire and Materials*, Vol. 28, 2004, pp. 269–280.



Peter WEISENPACHER studied theoretical physics at the Comenius University, Faculty of Mathematics and Physics, Department of Theoretical Physics, Bratislava, Slovakia and received his Ph.D. degree in 2003. He works as Research Scientist at the Slovak Academy of Sciences, Institute of Informatics, Department of Parallel Computational Methods and Algorithms. His current research interests include computational fluid dynamics, fire computer simulation and parallel computing. He participates in various research projects on fire simulation.



Jan GLASA graduated in numerical mathematics in 1986, received the his R.N.Dr. (Rerum Naturalium Doctor) degree in numerical mathematics and optimization methods and algorithms at the Comenius University in Bratislava, Slovakia and his C.Sc. degree (equivalent to Ph.D.) in computer science at the Slovak Academy of Sciences. He works for the Institute of Informatics, Slovak Academy of Sciences in Bratislava as Senior Scientist and serves as the head of the Scientific Council of the Institute. His current research interests include mathematical modelling and computer simulation of fires and parallel computing.



Ladislav HALADA graduated in mathematics in 1971, received his R.N.Dr. degree in mathematics and physics from the Faculty of Mathematics and Physics at the Comenius University in Bratislava, and his C.Sc. degree (equivalent to Ph.D.) in mathematics in 1982 from the same university. He is Associate Professor from 1991. During 1972–2001 he worked at different scientific institutions and universities in the Slovak Republic and also abroad. He is co-author of scientific books and numerous scientific papers.